Journal of Catalysis 272 (2010) 44–54

Contents lists available at ScienceDirect

Journal of Catalysis

journal homepage: www.elsevier.com/locate/jcat

The decisive role of the distribution of Al in the framework of beta zeolites on the structure and activity of Co ion species in propane–SCR–NO_x in the presence of water vapour

L. Čapek [1], J. Dědeček, P. Sazama, B. Wichterlová *

J. Heyrovský Institute of Physical Chemistry, Academy of Sciences of the Czech Republic, CZ-182 23 Prague 8, Czech Republic

ARTICLE INFO

Article history:
Received 21 January 2010
Revised 11 March 2010
Accepted 11 March 2010
Available online 24 April 2010

Keywords:
Co-beta zeolites
Al distribution
SCR–NO_x
NO_x streams with water vapour
UV–Vis of Co(II)

ABSTRACT

The role of the distribution of aluminium in the framework of beta zeolites in the formation of various types of counter Co species of different activity in C_3H_8–SCR–NO in the absence/presence of 10% water vapour was investigated. Different concentrations of Al atoms in the Al–O–$(Si–O)_2$–Al sequences in one ring (Al pairs) and isolated Al atoms in Al–O–$(Si–O)_{n>2}$–Al sequences located in two framework rings of parent BEA* zeolites were obtained by variation of the zeolite synthesis and by post-synthesis dealumination. Al atoms in the framework and their distribution were characterized by the combination of ^{29}Si MAS NMR of the parent BEA* zeolites and UV–Vis spectroscopy of the maximum-Co(II)-loaded BEA*. The concentration of Al pairs corresponded to the concentration of bare Co(II) ions in dehydrated maximum exchanged-Co(II)-BEA* calculated from the Vis spectra. Co-BEA* zeolites prepared by ion exchange from Co nitrate solution contained bare Co(II) ions balanced by Al pairs, which were formed preferentially, and "monovalent" Co-oxo species balanced by the isolated Al atoms. The relative concentration of bare Co(II) ions and Co-oxo species depends on the degree of Co(II) ion exchange and the concentration of Al pairs and isolated Al atoms in the zeolite framework. Superior activity was found with the counter Co-oxo species balancing isolated Al atoms, surviving even in wet (10% H_2O) NO_x streams. The bare Co(II) ions were active in dry NO_x streams, but their activity was negligible in wet NO_x streams. A highly active catalyst (more than twice than the other Co-BEA*) can be prepared by using a BEA zeolite containing a predominant concentration of isolated Al atoms in the framework.

1. Introduction

In addition to high structural stability and molecular shape selective properties of the pentasil ring zeolites of the MOR, FER, MFI and BEA* structures, metal ion species in these zeolites exhibit exceptional redox properties quite different from those located in aluminium-rich zeolites or supported on amorphous inorganic carriers (see e.g. [1–5]). This is manifested in numerous catalytic reactions, e.g. of NO decomposition and SCR–NO_x by hydrocarbons [6–12]. As the concentration of aluminium in these silicon-rich zeolites is low (Si/Al > 8), the local negative framework charge originated from the siting of aluminium atoms in the framework, which might exhibit various arrangements, can affect the properties of the counter metal ion species.

While the siting and coordination of bare divalent cations in MOR, FER, MFI and BEA* zeolite structures have been suggested [13–22] and widely accepted, there is a lack of information on the structure and properties of counter metal-oxo species in these zeolites. The studies employing various spectral and diffraction methods have not yet yielded clear identification and particularly quantitative analysis of these species (see e.g. [10,11,18,23,24]). An attempt is made here to elucidate the structure and concentration of the counter Co species in BEA* zeolites by using the Vis spectra of d–d transitions of bare Co(II) ions and the UV spectra of the charge transfer (CT) of the Co-oxo species. The Vis spectra of the d–d transitions of the maximum-Co(II)-exchanged beta zeolites combined with ^{29}Si MAS NMR are employed to estimate the distribution of aluminium atoms in the framework.

Selective catalytic reduction of NO_x (SCR–NO_x) by low paraffins over silicon-rich high-silica Co-zeolites, using methane and propane, has been shown to be a promising method for NO_x emission control in an oxidizing atmosphere from stationary sources [7,25–27]. However, the most important obstacle is preservation of the zeolite activity in real NO_x streams containing a high concentration (approx. 10%) of water vapour. It has been proven that the bare Co ions coordinated exclusively to the framework oxygen atoms of MFI, FER and MOR are highly active only in the absence of water

* Corresponding author.
E-mail addresses: libor.capek@upce.cz (L. Čapek), wichterl@jh-inst.cas.cz (B. Wichterlová).
[1] Present address: University Pardubice, Czech Republic.

0021-9517/$ - see front matter © 2010 Elsevier Inc. All rights reserved.
doi:10.1016/j.jcat.2010.03.013

vapour [1,28]. However, water vapour present in real exhaust gases substantially decreases the NO_x activity due to its adsorption on the Co ions [29].

With wet NO_x streams, only Co-BEA* catalyst with Co/Al of approx. 0.5 developed at ENI Technologie and OsakaGas Corp. was reported to exhibit long-term stable activity (>4000 h of time-on-stream) in SCR–NO_x using propane in 9% of water vapour [30–32]. At cobalt "over-exchange" loadings (Co/Al > 0.5), when Co oxide-like species supported on the zeolite can also be expected to occur, the SCR–NO_x activity was much lower. This suggests that the Co species that are highly active in C_3H_8–SCR–NO_x/H_2O are probably not bare exchanged Co ions or supported Co oxide-like species but represent specific structural counter Co species. The μ-oxo Co species in Co-BEA*, indicated by Raman spectra, were suggested to be such highly active sites [23,32]. However, their concentration in Co-BEA* was estimated to be rather low, much below the 10% of total Co concentration.

Later, we demonstrated that the high and stable C_3H_8–SCR–NO_x/H_2O activity (with 10% H_2O) on Co-BEA* zeolites was connected with a parent zeolite in which a high concentration of aluminium was preserved in the framework during template removal, in contrast to Co-BEA zeolites prepared from a partly dealuminated zeolite. The high activity of the former Co-BEA* catalyst was assigned to some cobalt-oxo species, which did not adsorb basic acetonitrile, in contrast to bare Co ions, and thus presumably also water molecules [11]. This suggests that the Al distribution in the framework could play an important role.

These findings and the results on the high redox activity of highly exchanged metallo-zeolites have increased an interest in analysis of the siting of aluminium in the framework of high-silica zeolites [33–44]. It also initiated our attempt in quantitative analysis of the relationship between the distribution of aluminium atoms in the framework and the structure and reactivity of the counter metallo-species [38,40]. However, complete analysis of Al occupation of the individual T sites in silicon-rich zeolites is not yet available.

Nevertheless, the low Al content in the framework and the high number of T sites in high-silica pentasil ring zeolites undoubtedly points to the variability of Al siting, from the viewpoint of both the occupation of the individual T sites and the local density of Al atoms. By using several sets of MFI zeolites with similar chemical composition, but synthesized under different conditions, we have shown that the Al siting in the framework is not random, not controlled by statistical rules, but it can be controlled kinetically by changing the chemical conditions of the zeolite synthesis [34,35,37,41,42].

In contrast to the Al siting in the framework T sites, the distribution of aluminium atoms in the framework with respect to the Al–O–Si–O–Al and Al–O–$(Si–O)_2$–Al sequences in one ring and isolated Al atoms occurring in two rings can be satisfactorily estimated by using ^{29}Si MAS NMR and the exchange capacity of bare Co(II) ions in the dehydrated zeolites [34,35]. ^{29}Si MAS NMR spectra provide a quantitative measure of the concentration of the Al–O–Si–O–Al sequences but cannot distinguish Al–O–$(Si–O)_2$–Al and isolated Al atoms in the framework. Nevertheless, the Al–O–$(Si–O)_2$–Al sequences in one ring can be determined indirectly from the exchange capacity of bare divalent cations (bonding exclusively to the framework oxygens) in dehydrated zeolites, obtained, e.g., from the quantitative analysis of the intensities of the d–d bands of the Vis spectra of Co(II) ions. Our results indicated that this type of Al distribution also depends on the conditions of the zeolite synthesis [34,35,37].

From the viewpoint of the counter divalent Co(II) species in dehydrated silicon-rich zeolites, these can occur as (i) bare divalent cations bonded exclusively to framework oxygen atoms neighbouring two Al atoms in the framework ring of a cationic site, (ii) μ-oxo, superoxo and peroxo Co species coordinated to two rings of define distance and each bearing an isolated Al atom and (iii) Co–O oxo species coordinated to one ring with one isolated Al atom. Finally, the zeolite can contain Co oxide-like undefined species supported on the zeolite, if the ion exchange is carried out at conditions that hydrolytic products are involved.

In this study, we would like to show that the state and activity of the counter Co species in Co-BEA* zeolites are decisively controlled by the adjacent local negative framework charge, which is represented by Al–O–$(Si–O)_2$–Al sequences or by isolated Al atoms. Moreover, we will, for the first time, show that the distribution of aluminium in beta zeolites can be controlled by their synthesis or post-synthesis treatment. To support the assumption about the effect of Al distribution on the activity of counter Co species, a comparison is made of the state and behaviour of Co species in beta zeolites differing in the distribution of framework aluminium in C_3H_8–SCR–NO_x in the presence and absence of water vapour. Various distribution of framework aluminium in the parent beta zeolites was obtained by using the following zeolite models: (i) a BEA* zeolite, where a very large amount of aluminium was preserved in the framework during template removal, which contained both Al–O–$(Si–O)_2$–Al sequences and isolated Al atoms, (ii) a dealuminated BEA* zeolite and a commercial sample, which appeared to contain a predominant concentration of Al–O–$(Si–O)_2$–Al sequences in the framework and (iii) a BEA* zeolite synthesized in the laboratory by using the procedure leading to a sample containing a predominant amount of framework aluminium as isolated Al atoms.

2. Experimental

2.1. Parent and Co-BEA* zeolites

Four parent BEA* zeolites were used, differing in the conditions of synthesis and template removal, in an attempt to obtain different distributions of Al in their frameworks. The distribution of aluminium atoms in the framework refers to the concentration of Al pairs, Al–O–$(Si–O)_{1\ or\ 2}$–Al sequences in one ring and isolated Al atoms (Al–O–$(Si–O)_{n>2}$–Al) located in two framework rings; for details, see the Discussion and Refs. [35,41,42,45]. In addition to the framework aluminium, some extra-framework aluminium was present in the dealuminated zeolite samples. The chemical composition of parent zeolites was obtained after their dissolution by using Atomic Absorption Spectrometry. Table 1 gives chemical composition of beta zeolites, concentration of Broensted and Lewis sites and distribution of framework aluminium between Al pairs and isolated Al atoms (see below).

Beta zeolite with Si/Al = 11.7 (BEA*) containing template (tetraethylammonium hydroxide) was kindly supplied by the Research Institute of Inorganic Chemistry, Unipetrol Inc., CZ. The synthesis corresponded to procedures performed on a large industrial scale. The zeolite denoted as H-BEA*-I was prepared from the as-synthesized BEA* sample by its calcination in an ammonia stream at 450 °C for 8 h to remove the template, according to the procedure first described by van Bekkum [46]. By such procedure, the NH_4^+ ions charge-balance and thus preserve aluminium in the framework. Before testing of the SCR–NO_x activity, the NH_4-form of this zeolite was deammoniated by calcination to yield the H-form. A zeolite denoted as H-BEA*-II was obtained from BEA* by removal of a template by zeolite calcination in an oxygen stream at 450 °C for 8 h. This procedure resulted in partial dealumination of the zeolite (see Table 1). Preparation of H-BEA*-I and H-BEA*-II samples was already described in [11] (denoted there as NH_4-BEA* and H-BEA*). The sample denoted as H-BEA*-III was a commercial substance kindly provided by PQ Corp., where detemplating was likely carried out on a large scale and substantial

Table 1
Chemical composition, concentration of Broensted and **Al-**Lewis sites and concentration of aluminium in the framework, aluminium pairs (Al_{pair}) and isolated aluminium atoms (Al_{isol}) of parent beta zeolites.

Zeolite	Si/Al	Al_{total} (mmol g^{-1})	Broensted sites, c_B[1] (mmol g^{-1})	Lewis sites, c_L[1] (mmol g^{-1})	Al_{FR} (mmol g^{-1})	Al_{pair}[2] (mmol g^{-1})	Al_{isol}[2] (mmol g^{-1})
H-BEA*-I	11.7	1.31	0.78	0.25	1.19	0.78	0.41
H-BEA*-II	11.5	1.33	0.24	0.49	0.78	0.70	0.08
H-BEA*-III	12.7	1.22	0.13	0.52	0.64	0.50	0.14
H-BEA*-IV	15.6	1.00	0.33	0.28	0.97	0.40	0.57

[1] Determined from quantitative analysis of IR spectra of adsorbed d_3-acetonitrile.
[2] Determined from the concentration of Co total and of quantitative analysis of Vis spectra of bare Co(II) ions balanced by Al pairs in dehydrated zeolites.

framework perturbation and dealumination occurred (see Table 1). The H-BEA*-IV zeolite was synthesized in our laboratory using a procedure providing beta zeolite differing substantially in the distribution of the aluminium in the framework compared to H-BEA*-I, -II and -III (see Table 1). The synthesis procedure is under patent application [47]. A template from the H-BEA*-IV zeolite was removed by calcination in a stream of dry nitrogen at 450 °C for 12 h, followed by calcination in a dry oxygen stream at 500 °C for 12 h.

IR spectra of skeletal vibrations, XRD, SEM and nitrogen adsorption (Fig. A and Table A of the Supplementary material) of the H-BEA*-IV sample (crystal size around 50 nm, specific surface area 544 $m^2\,g^{-1}$ and micropore volume 0.18 $cm^3\,g^{-1}$) indicated well-developed crystalline structure.

Co-BEA* zeolites with various Co concentrations were prepared by Co(II) ion exchange of the H-BEA*-I to -IV zeolites at RT with aqueous $Co(NO_3)_2$ solutions ranging in Co concentrations from 0.0001 to 0.10 mol l^{-1}. The developed procedure of Co ion exchange carried out at RT and with Co nitrate solutions of low concentrations excluded presence of hydrolytic products of Co(II) ions in both the solutions and Co-zeolites [18]. This was checked by Vis spectra (not shown) of the hydrated Co-zeolites and solutions with octahedrally coordinated Co(II) ions. Details of the Co ion exchange are given in Table B of the Supplementary material. After the Co(II) exchange, the zeolites were thoroughly washed several times with distilled water, filtered and dried in the open air. The chemical compositions of the Co-BEA* zeolites are given in Table 2.

2.2. Nuclear magnetic resonance

^{29}Si MAS NMR experiments were carried out on a Bruker Avance 500 MHz (11.7 T) Wide Bore spectrometer with 4 o.d. ZrO_2 rotors spun at a rotation speed of 5 kHz. A ^{29}Si MAS NMR high-power decoupling (HPDec) experiment with $\pi/4$ (1.7 μs) excitation pulse and relaxation delay 30 s and a cross-polarization (CP) experiment with 50% ramp CP pulse, contact time 2000 μs, high-power decoupling and relaxation delay 5 s was employed. ^{29}Si HPDec NMR spectra were decomposed to the Gaussian bands using Microcall Origin 4.1 software (Microcall Software Inc., USA). The framework aluminium content (Si/Al_{FR}) was estimated according to the formula

$$Si/Al_{FR} = I/0.25 \times I_1 \quad (1)$$

where I_1 denotes the intensity of the NMR line corresponding to the Si(3Si, 1Al) building unit, and I denotes the total ^{29}Si intensity, for details see Ref. [48].

2.3. UV–Vis–NIR diffuse reflectance spectroscopy

UV–Vis spectra of Co-BEA* zeolites were collected at RT after dehydration of the zeolites in a dynamic vacuum (10^{-3} Pa) at 450 °C for 3 h. The UV–Vis–NIR spectra were measured using a Perkin-Elmer Lambda 950 UV–Vis–NIR spectrometer equipped with a diffuse reflectance attachment with an integrating sphere coated by Spectralon™. Spectralon™ also served as a reference. The spectra were processed according to the Schuster–Kubelka–Munk equation

$$F(R_\infty) = (1 - F(R_\infty))^2/2R_\infty \quad (2)$$

The spectra were recorded under conditions provided for quantitative analysis of Co(II) species. After the baseline correction for absorption of the parent H-BEA* samples, the spectra in the region of the d-d transitions were simulated using Gaussian bands corresponding to the Co ions in the α-, β- and γ-type sites. The concentration of bare Co(II) ions in the zeolite was estimated using the absorption coefficients of Co ions in the α-, β- and γ- sites (11×10^{-3}, 7×10^{-3} and 5×10^{-3} cm^{-1} mmol g^{-1}, resp.). For more details on the spectral analysis and assignment of the individual bands to Co(II) sites, see Refs. [17,18].

2.4. FTIR spectroscopy

A Nicolet Magna-550 FTIR spectrometer with a MCT-B low-temperature detector was used to collect 200 scans at resolution of 2 cm^{-1} for a single spectrum. The samples were in the form of

Table 2
Chemical composition of Co-beta zeolites (Si/Al, Co/Al, Co_{total}) and concentration of Co ions balanced by Al pairs (Co_{2Al}) and isolated Al atoms (Co_{1Al}).

Zeolite	Si/Al_{total}	Co/Al_{total}	Co_{total} (wt.%)	Co_{total} (mmol g^{-1})	Co/Al_{FR}	Co_{2Al} (mmol g^{-1})	Co_{1Al} (mmol g^{-1})
Co-BEA*-I	12.8	0.19	1.37	0.23	0.20	0.23	0
Co-BEA*-I	11.5	0.30	2.33	0.40	0.33	0.30	0.10
Co-BEA*-I	11.9	0.50	3.66	0.62	0.52	0.36	0.26
Co-BEA*-II	14.0	0.22	1.43	0.24	0.31	0.24	0.00
Co-BEA*-II	13.1	0.32	2.17	0.37	0.47	0.35	0.02
Co-BEA*-III	13.0	0.05	0.35	0.06	0.10	0.06	0
Co-BEA*-III	13.6	0.16	1.06	0.18	0.30	0.18	0
Co-BEA*-III	14.0	0.25	1.61	0.27	0.46	0.25	0.02
Co-BEA*-IV	15.8	0.03	0.15	0.02	0.03	0.02	0
Co-BEA*-IV	16.4	0.28	1.57	0.27	0.27	0.20	0.07
Co-BEA*-IV	16.6	0.36	1.96	0.33	0.34	0.20	0.13
Co-BEA*-IV	16.7	0.45	2.41	0.41	0.42	0.20	0.21

self-supporting pellets with a thickness of about 5–10 mg cm^{-2} mounted in a carousel sample holder with six samples placed in a glass vacuum cell equipped with NaCl windows. For determination of the concentration of Broensted and Lewis sites, the FTIR spectra of the samples were measured at RT after their evacuation (10^{-3} Pa) at 450 °C and adsorption of d_3-acetonitrile at RT followed by evacuation for 20 min. The extinction coefficients for C≡N bonds on a Broensted site is $\varepsilon_B = 2.05 \pm 0.1$ cm μmol^{-1} and, for C≡N coordinated to Lewis site, equals $\varepsilon_L = 3.6 \pm 0.2$ cm μmol^{-1} (for details see Ref. [49]).

2.5. C_3H_8–SCR–NO_x in the absence and presence of water vapour in the feed

Reaction of C_3H_8–SCR–NO_x over parent and Co-BEA zeolites was carried out in a glass through-flow micro-reactor, typically with 400 mg of the catalyst. The reactor inner volume was filled with glass balls to minimize conversion of C_3H_8 in the gaseous phase prior to the catalyst bed. A reactant mixture consisting of 1000 ppm NO, 1000–3000 ppm C_3H_8, 2.5% O_2, 0 or 10% H_2O and the remainder consisting of He was kept at a total flow rate of 100 ml min^{-1} with corresponding GHSV 7500 h^{-1}. In selected cases, the reaction was measured at conditions of GHSV 15,000 and 30,000 h^{-1}. The catalyst was pretreated in an oxygen stream at 450 °C for 1 h. During this procedure, the NH_4-zeolites were deammoniated to H-zeolites under *in situ* conditions. The concentrations of NO and NO_2 in the inlet and outlet of the reactor were continuously monitored by an NO/NO_x chemiluminescence analyzer (VAMET-CZ). The concentrations of C_1–C_3 hydrocarbons, CO_2, CO and N_2O were provided by an on-line-connected Hewlett Packard 6090 gas chromatograph (for more details see Ref. [50]). No N_2O was detected in the products. For most of the tests, the selectivity of NO conversion to N_2 was >98% (the rest was NO_2). Propane was transformed to CO_2 with 70% selectivity; the rest was CO. The effect of the presence (10 vol.%) and absence (0 vol.%) of water vapour in the feed was investigated depending on the reaction time-on-stream (TOS) with preservation of constant concentrations of NO_x (1000 ppm), O_2 (2.5 vol.%) and propane (1000 ppm) at 350 °C and GHSV 7500 h^{-1} or 30,000 h^{-1}. The NO_x conversions are reported after TOS of about 1 h. At a given temperature, the conversion of NO_x both in the presence and in the absence of water vapour increased steadily and reached a stable value. For Co-BEA*-IV and in some experiments for Co-BEA*-I, the NO_x conversion changed surprisingly after switching on/off of water vapour (10 vol.%) in the feed. Therefore, behaviour of these zeolites with TOS was investigated in more detail.

3. Results

3.1. State and distribution of Al in the framework

The ^{29}Si MAS NMR spectra of H-BEA*-III and -IV parent zeolites and their analysis are shown in Fig. 1. Resonances between −97.9 and −101.7 ppm can be attributed according to the cross-polarization experiment (not shown in the figures) to the Si(2Si, 2OH) and Si(3Si, 1OH) species. Resonances between −103.0 and −107.4 ppm correspond to the Si(3Si, 1Al) atoms, and resonances above −108 ppm reflect Si(4Si) atoms. These findings indicated that Si neighbours on only one Al atom, and thus, no Al–O–Si–O–Al sequences are present in these parent zeolites. ^{29}Si MAS NMR spectra of H-BEA*-I and -II reported in Ref. [11] also showed that the Al–O–Si–O–Al sequences in these zeolites were not present. This implies that only Al–O–(Si–O)$_2$–Al sequences as Al pairs and isolated Al atoms (Al–O–(Si–O)$_{n>2}$–Al sequences) occur in the frameworks of the studied zeolites.

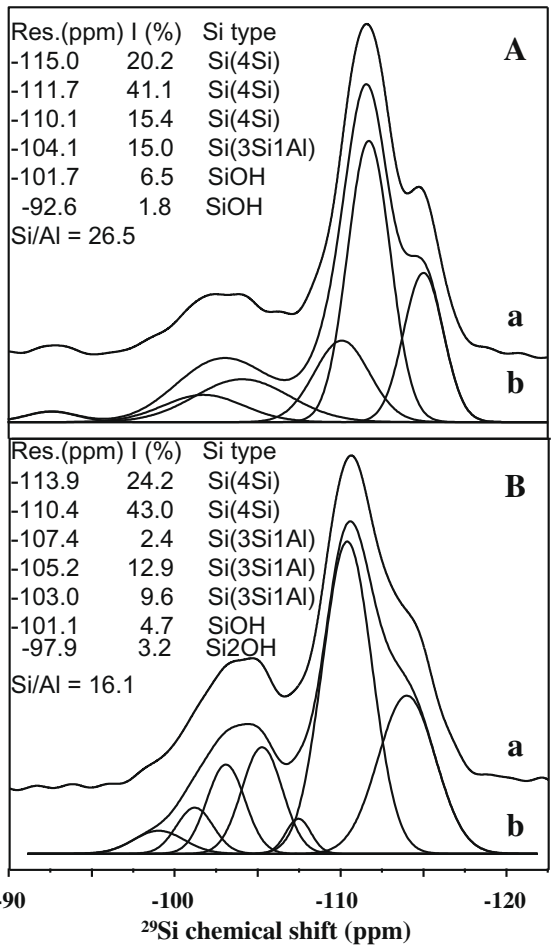

Fig. 1. ^{29}Si MAS NMR spectra of BEA*-III (A) and BEA*-IV (B). Experimental spectra (a) and spectra simulations (b).

From the quantitative analysis of the ^{29}Si MAS NMR spectra of hydrated parent beta samples (Fig. 1 and Ref. [11]), it follows that the concentration of extra-framework Al atoms is negligible in H-BEA*-I and H-BEA*-IV (less than 10%), but nearly 50% of extra-framework Al atoms are present in partly dealuminated H-BEA*-II and H-BEA*-III, see Table 1. The dealumination of the framework of H-BEA*-II occurred during template removal by zeolite calcination.

Nevertheless, quantitative analysis of the FTIR spectra of d_3-acetonitrile adsorbed on the parent dehydrated beta zeolites (for details of the analysis, see Ref. [49]) and the spectra analysis given in Ref. [11] revealed a non-negligible amount of Al-Lewis sites in addition to the Broensted sites in all the dehydrated zeolites (Table 1). This finding is in agreement with the well-known fact that a substantial perturbation of the framework at Al sites takes place in dehydrated H-BEA* zeolites [51,52] (see Table 1) reflecting in formation of "framework" Al-Lewis sites, which remain to be located in the framework T sites.

As the concentration of the Al atoms in Al–O–(Si–O)$_2$–Al sequences and the isolated Al atoms cannot be determined by ^{27}Al MAS NMR analysis [36,42], we used the methodology for estimation of the concentration of Al pairs in the framework by using the highest exchange degree of bare Co(II) ions in dehydrated zeolites. These values were calculated from the intensity of the d–d transitions of bare Co(II) ions in the cationic sites of dehydrated BEA* zeolites and the corresponding absorption coefficients for the individual Co(II) ions taken from Ref. [18] (see further in Fig. 2 and Table 2). The highest concentration of bare Co(II) ions

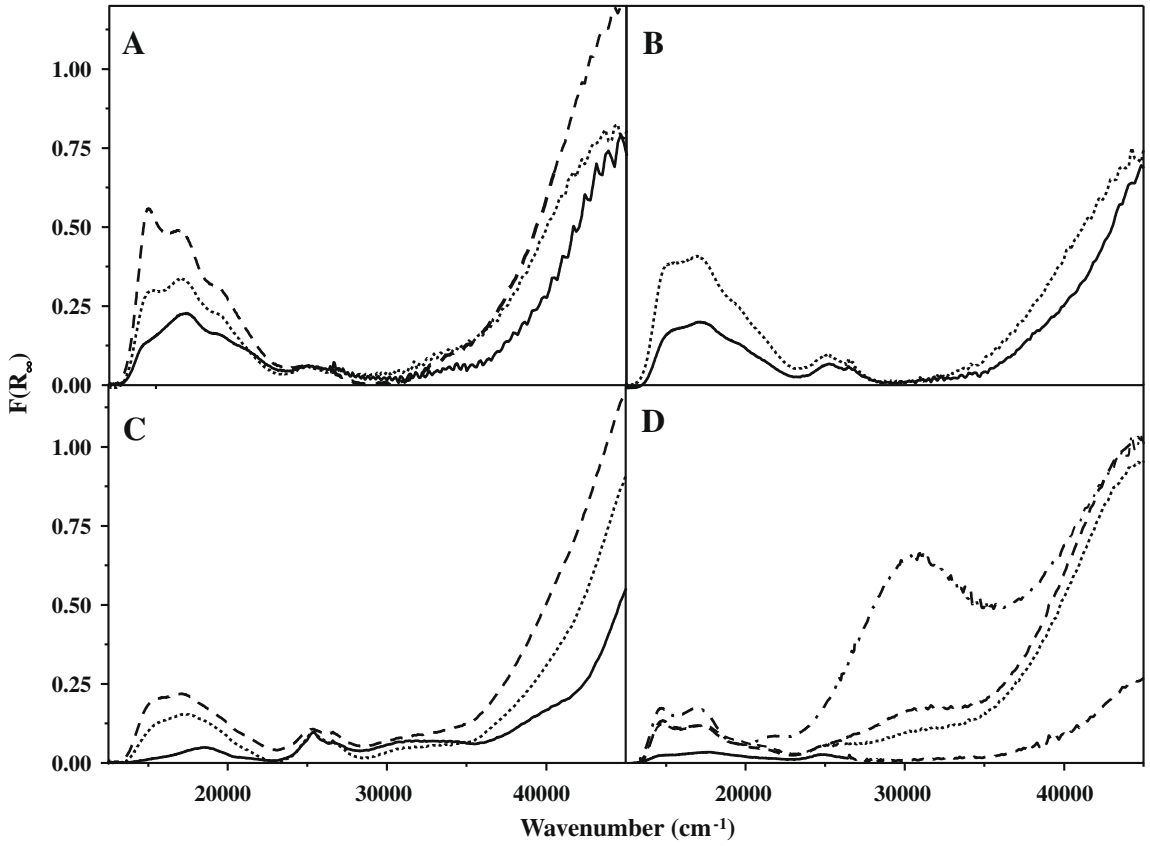

Fig. 2. UV–Vis spectra of Co-BEA*-I (A) with Co/Al 0.19 (————), 0.30 (- - - - -) and 0.50 (– –); Co-BEA*-II (B) with Co/Al 0.22 (———) and 0.32 (- - - - -); Co-BEA*-III (C) with Co/Al 0.05 (———), 0.16 (- - - - -) and 0.25 (– –); and Co-BEA*-IV (D) with Co/Al 0.03 (———), 0.28 (- - - - -), 0.36 (– –) and 0.45 (— - —).

Table 3
Composition and TOF_{total} and TOF_{1Al} values for Co-beta zeolites in C_3H_8–SCR–NO_x/H_2O in 10% H_2O at 350 °C and GHSV 7500 and 30,000 h^{-1}.

Catalyst	Co/Al	Co (wt.%)	Al_{FR} (mmol g^{-1})	Al_{isol} (mmol g^{-1})	Co_{1Al} (mmol g^{-1})	GHSV					
						7500 h^{-1}			30,000 h^{-1}		
						N_2 yield (%)	TOF_{total} (h^{-1})	TOF_{1Al} (h^{-1})	N_2 yield (%)	TOF_{total} (h^{-1})	TOF_{1Al} (h^{-1})
Co-BEA*-I	0.19	1.37	1.19	0.41	0	0.0	0.00	0.00			
Co-BEA*-I	0.30	2.33	1.19	0.41	0.10	31.7	0.49	2.0			
Co-BEA*-I	0.50	3.66	1.19	0.41	0.26	88.2	0.87	2.2	40.3	1.59	3.9
Co-BEA*-II	0.22	1.43	0.78	0.08	0.00	14.6	n.d.	n.d.			
Co-BEA*-II	0.32	2.17	0.78	0.08	0.02	20.7	0.34				
Co-BEA*-III	0.05	0.35	0.59	0.14	0	19.9	n.d.	n.d.			
Co-BEA*-III	0.16	1.06	0.59	0.14	0.00	15.0	n.d.	n.d.			
Co-BEA*-III	0.25	1.61	0.59	0.14	0.02	10.9	0.24				
Co-BEA*-IV	0.28	1.57	0.97	0.59	0.07	37.5	0.87	3.4			
Co-BEA*-IV	0.36	1.96	0.97	0.59	0.13	89.0	1.64	4.2			
Co-BEA*-IV	0.45	2.41	0.97	0.59	0.21	90.7	1.36	2.7	31.4	1.86	3.6

TOF_{total} and TOF_{1Al} were not calculated for Co_{1Al} concentrations <0.02 mmol g^{-1}.

in Co-BEA* zeolites corresponds to the concentration of Al pairs, Al–O–(Si–O)$_2$–Al sequences, in one ring in the zeolite; these values are denoted in Tables 1–3 as Co_{2Al} and Al_{pair} for the concentrations of bare Co(II) ions and the Al atoms in the Al–O–(Si-O)$_2$–Al sequences, respectively. The concentrations of isolated Al atoms in the framework (Al_{isol}) were calculated as the difference in the concentrations of framework aluminium (Al_{total}), obtained from the ^{29}Si MAS NMR spectra of the hydrated zeolites, and the concentrations of Al atoms in the Al pairs, Al–(Si–O)$_2$–Al sequences. The results are summarized in Tables 1 and 2.

The concentrations of Al atoms in Al–O–(Si–O)$_2$–Al sequences located in one ring and of the isolated Al atoms in the two framework rings are given in Table 1. In the H-BEA-I sample, approx. 65% of the Al atoms are located in Al–O–(Si-O)$_2$–Al sequences. Both dealuminated H-BEA*-II and H-BEA*-III zeolites contain far fewer isolated Al atoms, and the Al–O–(Si–O)$_2$–Al sequences greatly predominate in their frameworks, containing approx. 90% and 80% Al in the Al–O–(Si–O)$_2$–Al sequences, respectively. As both H-BEA*-I and H-BEA*-II originated from the same beta (Si/Al 11.7) sample, it follows that the BEA* zeolite was preferably dealuminated by removing isolated Al atoms from the framework. In contrast, the H-BEA*-IV sample, synthesized by a specific procedure presumably to yield a high concentration of isolated Al atoms in the framework, exhibited above 60 rel.% of framework aluminium as isolated Al atoms.

3.2. Co species in Co-BEA* zeolites

Co(II) ions were exchanged into the parent beta zeolites from Co nitrate solutions at conditions (the conditions are given in Table B of the Supplementary material), where Co(II) hexaquo-complexes greatly predominated as follows from UV–Vis spectra (not shown). These Co(II) complexes in hydrated zeolites might be charge-balanced by Al pairs or by two "close" isolated framework Al atoms. However, after dehydration of Co-zeolites, bare Co(II) ions (coordinated only to framework oxygens) are bound in the cationic sites balanced by Al–O–(Si–O)$_2$–Al sequences. The Co(II) ions previously balanced by "close" isolated Al atoms in hydrated zeolites might be balanced by an isolated framework Al atoms as Co–O species or by two isolated Al atoms located in two rings as Co–O$_x$–Co species.

Fig. 2A–D depicts the UV–Vis spectra of the dehydrated Co-BEA*-I, -II, -III and -IV zeolites in dependence on the Co concentration. For the details of spectra deconvolution and attribution of the individual UV–Vis bands to various Co ion species and corresponding absorption coefficients, see Ref. [18]. The bands in the 14,000–22,000 cm^{-1} region reflect the d–d transitions of the bare Co(II) ions coordinated at the α, β and γ cationic positions exclusively to the framework oxygen atoms. The band at 14,700 cm^{-1} reflects the Co ions in the α cationic sites, a relatively intense quartet of bands at 15,500, 16,300, 17,500 and 21,700 cm^{-1} corresponds to the presence of the most populated Co(II) ions at the β sites and the low intense doublet at 18,900 and 20,100 cm^{-1} belongs to the Co(II) ions at the γ cationic sites. The analysis of Vis spectra of maximum loaded Co-BEA*-I and -IV is demonstrated in Fig. 3. The concentrations of bare Co(II) ions balanced by Al pairs (Co_{2Al}) in all the samples are given in Table 2.

The broad band with maximum at 31,500 cm^{-1} obtained only for Co-BEA*-IV (see Fig. 2D) could be attributed to the charge-transfer transition of the μ-oxo, superoxo or peroxo Co species [18]. It should be noted that not all the Co-oxo species that are potentially possibly present in zeolites exhibit CT transitions below 50,000 cm^{-1}. There might be Co-oxo species without a CT transition observable by diffuse reflectance spectroscopy, and their presence in our Co-BEA* samples is indicated from the chemical analysis of cobalt in Co-zeolites and the calculated concentration of Co(II) ions attached to isolated Al atoms (see Table 2 and the Discussion). This assumption is supported by a possible CT transition above 50,000 cm^{-1}. It should be mentioned that we did not detect transitions of Co oxide-like species for any of the dehydrated Co-BEA* zeolites. The strong CT bands with maximum around 45,000 cm^{-1}, observed for all the Co-BEA* zeolites and of high intensity for zeolites with high concentration of bare Co(II) ions (Fig. 2A–D), were attributed to the CT between the skeletal oxygen atoms and the exchanged Co(II) ions, i.e. to the bonding of the Co ions to the framework oxygen atoms.

For all the Co-beta zeolites, differing in the concentrations of Al atoms in the Al pairs and isolated Al atoms, the intensity of the d–d bands attributed to the bare exchanged Co(II) ions increased with increasing concentration of Co. Co-BEA*-I exhibited the highest intensity of the absorption in the 14,000–22,000 cm^{-1} region, indicating the highest concentration of Co_{2Al} cations. The lowest intensity of the d-d bands, moreover, saturated at low Co loadings (Co_{2Al} 0.2 mmol g^{-1}), was found for Co-BEA*-IV. Table 2 summarizes the estimated concentrations of bare Co ions balanced by framework Al–O–(Si–O)$_2$–Al sequence.

For the Co-BEA*-IV zeolites, containing predominant concentration of framework aluminium as isolated Al atoms (61% of total Al, see Table 1), a much lower absorption intensity was found in the region of d–d transitions, but in contrast, an intense broad CT band at 31,500 cm^{-1}, possibly of some counter Co-oxo species, was observed (Fig. 2D). The intensity of the latter broad band increased particularly for loadings Co/Al$_{FR}$ > 0.3. It should be pointed out that no such distinct CT band was observed for the Co-BEA*-I, -II and -III zeolites.

The UV–Vis results, showing the d–d transitions of bare Co(II) ions and CT bands of Co(II)–O$_{FR}$ and Co-oxo species with extra-framework oxygen atoms, indicated that only counter Co ion species are present in dehydrated with extra-framework oxygens Co-BEA* zeolites. This conclusion is confirmed by the absence of Raman bands (679, 514 and 472 cm^{-1}) of Co oxide-like species in dehydrated Co-BEA* zeolites (for illustration, see the spectrum of Co-BEA-I Co/Al 0.50 in Fig. B of the Supplementary material).

As the extinction coefficient of the broad CT band at 31,500 cm^{-1} is approx. 50 times higher compared to that of the d–d transitions, the concentration of the counter Co-oxo species would be low, but not possible to be estimated. However, we do not suppose that all Co-oxo species have to exhibit a CT band in the region of the recorded UV–Vis spectra.

Nevertheless, the presence only of counter Co ion species in the studied Co-beta zeolites gives us an opportunity to analyze quantitatively the Co-oxo species balanced by isolated Al atoms in the framework. The concentration of Co_{1Al} was calculated as the difference between the total concentration of Co(II) ions (Co_{total}) and the concentration of Co(II) ions balanced by the Al pairs, Co_{2Al} (see

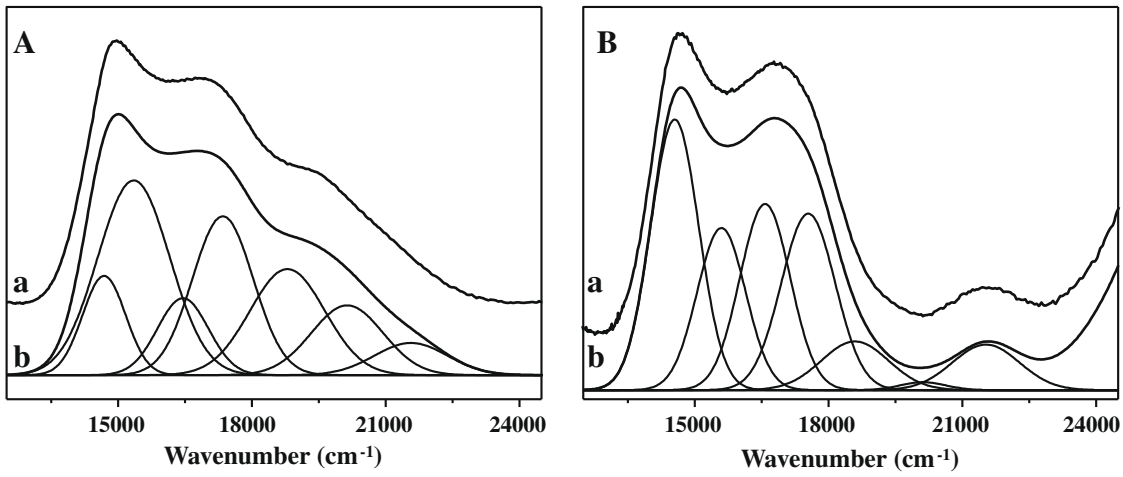

Fig. 3. Analysis of Vis spectra of Co-BEA*-I Co/Al 0.50 (A) and Co-BEA*-IV Co/Al 0.45 (B). Experimental spectra after baseline subtraction (a) and spectra simulations (b). Calculated Co concentration for (A) Coα = 0.07, Coβ = 0.23, Coγ = 0.06 and total Co = 0.36 mmol g^{-1}. Calculated Co concentration for (B) Coα = 0.05, Coβ = 0.13, Coγ = 0.02, and total Co = 0.20 mmol g^{-1}.

Table 2). The estimated error for Co_{2Al}, Co_{1Al} and related Al_{pair}, Al_{isol} values is <±10 rel.%.

From Table 2 (two last columns) it can be seen that with increasing Co loadings for all the Co-BEA* zeolites, the Co ions first occupy sites adjacent to the Al pairs in the cationic sites (Co_{2Al}), while isolated Al atoms are subsequently occupied by "monovalent" Co-oxo species (Co_{1Al}) – last column. This is caused by the conditions of the Co ion exchange, where the solution contained highly predominated hexaquo-complexes of Co(II) ions to guarantee complete Co(II) exchange at the cationic sites with Al pairs. Therefore, the Co ions adjacent to Al_{isol} could be formed in hydrated zeolites only at sites where isolated framework Al atoms located in two rings are close enough to balance the divalent Co(II) hexaquo-complex present.

3.3. C_3H_8–SCR–NO_x of Co-BEA* zeolites in the absence and presence of water vapour (10 vol.%) in the feed

Fig. 4A–D depicts the dependence of the N_2 yield and conversion of propane on the Co concentration in the presence and absence of water vapour in the feed over Co-BEA* zeolites plotted at 350 °C, where the activity is the most sensitive to the temperature. The effect of the Co concentration on SCR–NO_x is expressed in wt.% (Fig. 4) as well as in Co/Al_{FR} (Fig. 5).

All four parent dehydrated H-BEA* zeolites possessed considerable SCR–NO_x activity. This is because the dehydrated zeolites exhibit high concentration of Al-Lewis sites in addition to Broensted sites (see Table 1), as has been generally observed [51]. The concentration of Al-Lewis sites depends on the synthesis procedure and post-synthesis treatment. Some of the Al-Lewis sites are represented by perturbed framework Al atoms; this perturbation is removed by the exchanged Co(II) ions. Nevertheless, some of these extra-framework Al-Lewis sites, present mainly in partly dealuminated H-BEA*-II and H-BEA*-III zeolites, remain unaltered. Considering the concentration of Al-Lewis sites in the parent zeolites (Table 1), it follows that the Al-Lewis sites are connected with the SCR–NO_x activity in the absence of water vapour in the feed, being the lowest for H-BEA*-I and H-BEA*-IV and the highest for H-BEA*-II and H-BEA*-III (see Table 1 and Figs. 4 and 5). However, the Al-Lewis sites are blocked in the presence of water, resulting in the low activity of all the parent zeolites. We do not assume that Al-Lewis sites are the only active sites for SCR–NO_x, but most likely, they function in cooperation with the trace concentration of Fe present in the zeolites, as suggested in Ref. [53].

The above results imply that the activity of Co-BEA* zeolites in SCR–NO_x in the absence of water vapour is substantially affected by the replacement of Al-Lewis sites by Co ions and, accordingly, the activity of the Co ions in beta zeolites at low Co concentrations is almost impossible to evaluate. Therefore, the results of the effect of water vapour on the SCR–NO_x activity are discussed for $Co/Al_{FR} > 0.3$, where most of the "framework" Al-Lewis sites have already been removed by the exchanged Co ions.

Investigation into Co-beta zeolites with frameworks of different concentrations of Al pairs and isolated Al atoms, and of bound

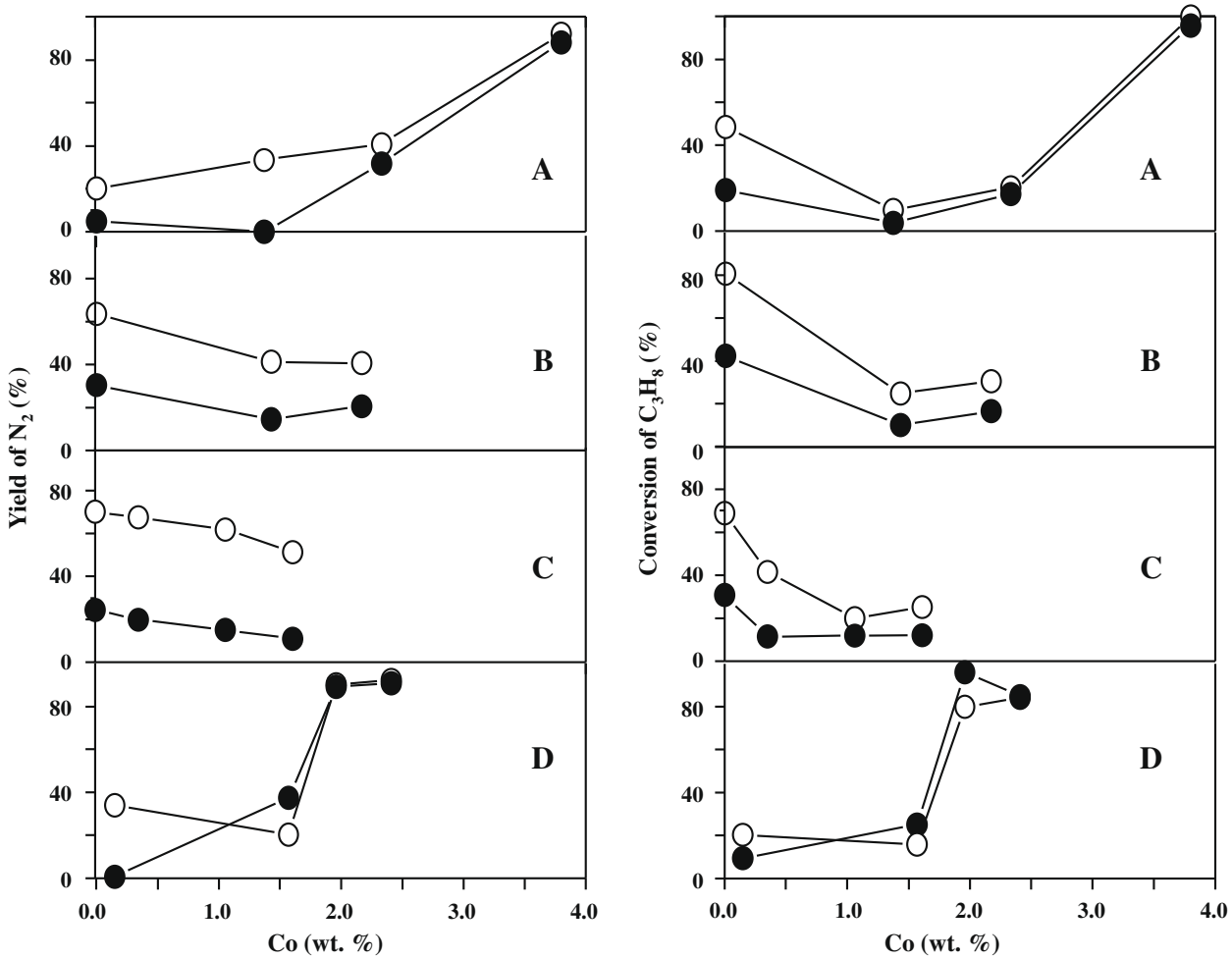

Fig. 4. The dependence of N_2 yield and C_3H_8 conversion in SCR–NO_x under presence (●) and absence (○) of water vapour over Co-BEA*-I (A), Co-BEA*-II (B), Co-BEA*-III (C) and Co-BEA*-IV (D) on Co concentration at 1000 ppm NO, 1000 ppm C_3H_8, 2.5% O_2, 0 or 10% H_2O and rest He, at 350 °C and GHSV 7500 h^{-1}.

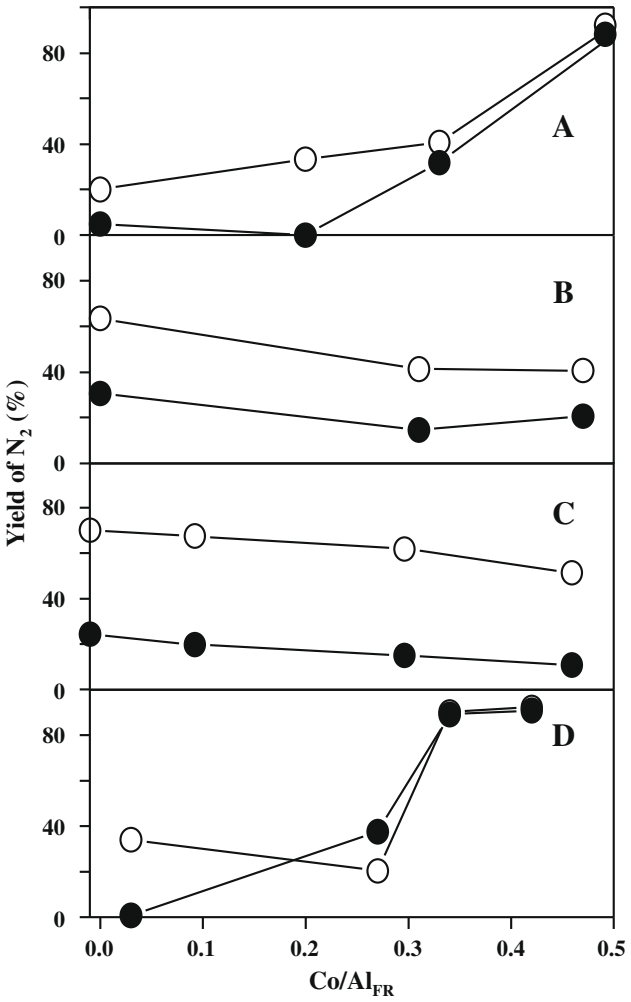

Fig. 5. The dependence of N_2 yield in SCR–NO_x under presence (●) and absence (○) of water vapour over Co-BEA*-I (A), Co-BEA*-II (B), Co-BEA*-III (C) and Co-BEA*-IV (D) on Co/Al_{FR} at 1000 ppm NO, 1000 ppm C_3H_8, 2.5% O_2, 0 or 10% H_2O and rest He, at 350 °C and GHSV 7500 h^{-1}.

counter Co species (Co_{2Al} and Co_{1Al}), enabled comparison of their activities. It should be stressed that the Co-BEA*-IV with a high relative concentration of isolated Al atoms in the framework exhibited much higher activity after Co loading (already at approx. 2.0 wt.%) compared to the other Co-zeolites (Figs. 4 and 5) in both the presence and absence of water vapour. This indicates the presence of some highly active Co species in this zeolite.

In the absence of water vapour in the feed, the dealuminated Co-BEA*-II and -III zeolites with high relative concentrations of Al pairs and thus high relative concentrations of bare Co(II) ions and extra-framework aluminium exhibited decreased NO_x and propane conversion levels with the increasing Co loadings. This indicates that Al-Lewis sites in cooperation with Fe species under dry conditions yield higher activity compared to the Co ions. The SCR–NO_x activity of Co-BEA*-I increased considerably with increasing Co loading at Co/Al > 0.3. Similar behaviour in the absence of water vapour with varying Co concentration was found with Co-BEA*-IV, but the sharp increase in activity occurred at much lower Co loadings (cf. Table 3 and Figs. 4D and 5D). This shows that at higher Co loadings, both Co-BEA*-I and Co-BEA*-IV contained highly active Co ions, but the activity of the Co-BEA*-IV zeolites at similar Co concentrations was much higher.

Quite different behaviour of the individual Co-beta zeolites was observed when water was added to the feed (SCR–NO_x/H_2O) – empty points in Figs. 4 and 5. The activity of Co-BEA*-I decreased only slightly (approx. 5%) and was stable for several hours. The activity of both dealuminated zeolites after addition of water decreased immediately and substantially, and then the conversion was stable. In contrast, the activity of Co-BEA*-IV in water vapour was high at much lower Co loadings compared to that of Co-BEA*-I. At 2.0 wt.% Co, the Co-BEA*-IV already exhibited conversion above 90%, which was attained with Co-BEA*-I at a loading of approx. 3.8 wt.% Co. It is to be noted that the N_2 yield increased up to Co/Al_{FR} close to 0.5, indicating contribution of counter Co ions to the SCR–NO_x/H_2O activity.

However, the behaviour of Co-BEA*-IV with TOS after addition and removal of water vapour from the stream in long TOS was surprising. In the absence of water, the NO_x conversion was stable for TOS of approx. 3 h (Fig. 6 – empty points), but then the conversion decreased within 0.5 h and was again stable. If water vapour was added to the stream, the short decrease in the activity was followed by a substantial enhancement in the NO_x and propane conversion. These effects were quite reversible with addition/removal of water to/from the feed; moreover, they were more pronounced with increasing Co loadings in Co-BEA*-IV (Fig. 6). It should be noted that no significant change in the selectivity of the reaction was observed.

While no changes in NO_x conversion were observed in switching water vapour on/off in the feed over Co-BEA*-I under conditions of the standard test (Figs. 4 and 5), when the concentration

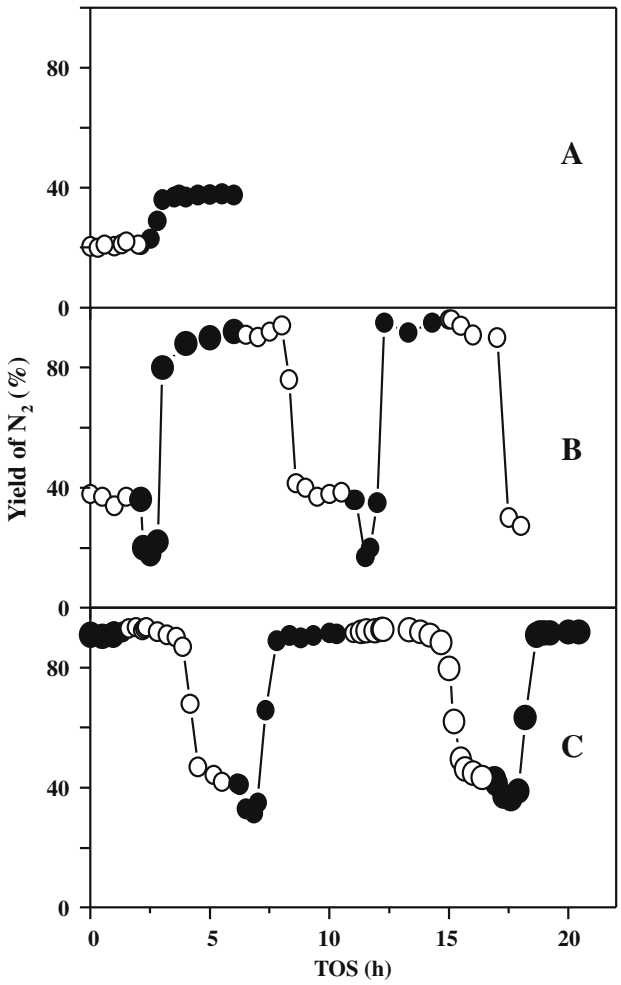

Fig. 6. Transient behaviour in TOS in SCR–NO_x of Co-BEA*-IV depending on Co concentration and presence (●) and absence (○) of H_2O at 1000 ppm NO, 1000 ppm C_3H_8, 2.5% O_2, 0 or 10% H_2O and rest He, at 350 °C and GHSV 7500 h^{-1}.

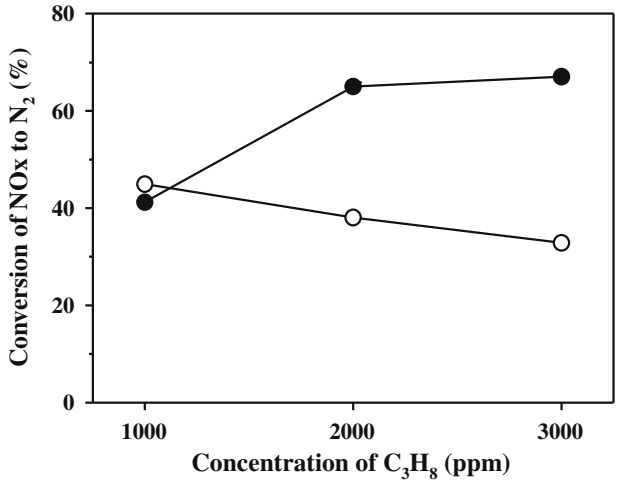

Fig. 7. Effect of the presence (●) and absence (○) of water vapour in the feed on conversion of NO_x to N_2 over Co-BEA*-I Co/Al = 0.50 depending on propane concentration of 1000–3000 ppm C_3H_8, 2.5% O_2, 0% H_2O or 10% H_2O and He at 350 °C and GHSV 15,000 h^{-1}.

of propane was increased from 1000 up to 3000 ppm, a similar transient increase in NO_x conversion was observed in the presence of water like with the Co-BEA*-IV sample (Fig. 7). At higher propane concentrations, the NO_x conversion was substantially increased from approx. 40% to 65% and from approx. 35% to 67%. These results indicate that the conditions (propane concentration) of the complex SCR–NO_x process greatly influence the effect of water vapour on the NO_x conversion.

To compare the efficiencies of various types of counter Co ion species present in the individual Co-BEA* zeolites in SCR–NO_x/H_2O, the values of the turn-over frequency (TOF) per Co_{total} atom at SCR–NO_x/H_2O were calculated. It follows from Table 3 that for the dealuminated Co-BEA*-II and Co-BEA*-III zeolites containing greatly predominating concentrations of Co(II) ions balanced by Al pairs (>90%), the TOF_{total} values (per total Co) are at maximum Co loading low, with TOF_{total} 0.34–0.24 h^{-1}, respectively. Increasing TOF_{total} values from 0.5 to 0.9 h^{-1} are found with the increasing Co loadings for Co-BEA*-I, but the highest TOF_{total} values are exhibited by Co-BEA*-IV, where Co species reached TOF_{total} from 0.9 to 1.4 h^{-1}.

The TOF_{total} results indicate that Co-BEA*-IV and Co-BEA*-I contain the most active Co species at higher Co loadings. If the TOF values were calculated per Co species adjacent to an isolated Al atom in the framework (Co_{1Al}), under the assumption that the bare Co(II) ions practically do not contribute to the C_3H_8-SCR–NO_x/H_2O activity (see Table 3), the TOF_{1Al} values of 2.2 and 3.4–4.2 h^{-1} were obtained for Co-BEA*-I and Co-BEA*-IV, respectively. It should be mentioned that similar TOF value per active Co species (TOF approx. 2.3 h^{-1}) at the same reaction conditions was obtained in our previous study on the Co-BEA*-I zeolite, denoted there as $CoNH_4$-BEA [11]. In that study, the highly active species were identified as Co-oxo species not adsorbing acetonitrile and thus presumably also water molecules at the SCR–NO process.

As the TOF values were calculated at 7500 h^{-1} using high NO_x conversions, we tested the most active Co-BEA*-I and Co-BEA*-IV, also at GHSV 30,000 h^{-1}. With NO_x conversions of 40% and 31%, respectively, the TOF_{total} and TOF_{1Al} values were reasonably close for these samples; TOF_{total} 1.6 and 1.9 h^{-1}, and TOF_{1Al} 3.6 and 3.9 h^{-1}, respectively.

4. Discussion

Discussions have long been held on the state and reactivity of divalent cation species in silicon-rich zeolites, particularly those with metal/Al ⩾ 0.5 [6,7,25,30,32,54–56]. To attain such values, metal acetate solutions are frequently used, providing "monovalent" species for the ion exchange. However, quantitative analysis of the obtained metal-oxo species, enabling relationship between their concentration and activity, has so far failed, even though numerous spectral and diffraction techniques have been used [5,6,23,25,27,55].

With respect to Co-BEA* zeolites, in addition to bare Co(II) ions coordinated exclusively to framework oxygen atoms and adjacent to two Al atoms in the ring of the cationic site, the presence of Co–O, bridged Co–O–Co and μ-oxo, peroxo and superoxo Co species should be considered. The Raman band around 600 cm^{-1} observed in the Co-BEA* with Co/Al close to 0.5 and exhibiting stable NO_x conversion in C_3H_8–SCR–NO_x/H_2O [23] was attributed to a low concentration of μ-oxo Co(II) species. But their quantitative analysis was not done.

Our long attempt to obtain direct quantitative analysis of the complex Co-oxo species by UV–Vis failed, as not all Co-oxo species, potentially present in zeolites, exhibit CT transitions below 50,000 cm^{-1}. There is no quantitative direct experimental information on the defined Co-oxo species, and generally on metal-oxo structures in beta and also other pentasil ring zeolites.

Therefore, to achieve quantitative analysis of Co-oxo species and to analyze the effect of local negative framework charge on the structure and reactivity of counter Co species, we attempted to employ model beta zeolites with quite different distribution of aluminium atoms in the framework and thus presumably different counter Co(II) species to identify their concentrations and related activities. By using a background of knowledge on the distribution of aluminium atoms in the MFI framework depending on the conditions of the zeolite synthesis [34,35,37], the following parent beta zeolites were prepared and their Co-forms used: (i) a BEA* zeolite, where a vast amount of aluminium in the framework was preserved during template removal, which contained both Al pairs and isolated Al atoms in the framework, (ii) a dealuminated zeolite and a commercial beta sample, which thereafter appeared to contain highly predominating concentration of Al pairs in the framework, and (iii) a BEA* zeolite synthesized in the laboratory using a procedure yielding a sample containing a predominant amount of the framework aluminium as isolated Al atoms.

As the ^{29}Si MAS NMR spectra indicated the absence of Si(2Si, 2Al) atoms and thus the absence of the Al–O–Si–O–Al sequences in the framework of all the studied beta zeolites (cf. Fig. 1 and Ref. [11]), it was clear that the zeolites can contain only Al–O–$(Si–O)_2$–Al sequences in one ring and isolated Al atoms with Al–O–$(Si–O)_{n>2}$–Al sequences in different rings. However, ^{29}Si MAS NMR cannot distinguish these latter sequences nor can ^{27}Al MAS NMR spectra. Therefore, to distinguish Al–O–$(Si–O)_2$–Al sequences and isolated Al atoms in the framework, we must use a method based on the assumption that the Al–O–$(Si–O)_2$–Al sequences in one ring can be quantitatively balanced by bare Co(II) ions bonded in dehydrated fully exchanged zeolites exclusively to framework oxygens [34,35]. A necessary condition for obtaining quantitative analysis of the concentration of Al–O–$(Si–O)_2$–Al sequences in one ring is the complete charge-balance of all these sequences by bare Co(II) ions (see Table 2). Additional Co(II) ion species exchanged into beta zeolites (see Table 2, difference between Co_{total} and Co_{2Al}, in the absence of Co oxide entities) should be exchanged as Co(II)–O or bridged Co–O_x–Co complexes, balanced by one or two isolated framework Al atoms, respectively, located in two rings.

Co-BEA-II and Co-BEA-III exhibited the highest relative concentrations of bare Co(II) ions related to the concentration of Al in the framework (approx. 90%, see Tables 1 and 2), as calculated from the Vis intensities of the d–d bands of bare Co(II) ions, and thus of the Al pairs in one ring. This indicates that the dealumination

of beta zeolites occurred predominantly by the removal of isolated Al atoms from the framework. On contrary, the low intensity of the Vis bands of the d–d transitions of bare Co(II) ions in the synthesized H-BEA*-IV (Fig. 2D) reflected a much lower relative concentration of Al in the Al pairs and thus a high concentration of isolated Al atoms (60%, see Tables 1 and 2).

As mentioned above, a straightforward identification of the Co-oxo species by spectral methods is not possible. The broad intense CT band at 31,500 cm^{-1}, increasing with the Co concentration in Co-BEA*-IV, could be ascribed to some Co-peroxo, -superoxo or μ-oxo Co(II) counter species (Fig. 2D) [57–59]. The absorption coefficient of this CT band was suggested to be approx. 50 times higher compared to that of the d–d transitions [11]. It follows that the intensity of the observed CT band at 31,500 cm^{-1} reflects only a low concentration of Co-oxo species. Moreover, for Co-BEA*-I, the intensity of absorption in this region increased only slightly and did not correspond to the expected concentration of Co-oxo species that followed from chemical analysis. These findings imply that either a very small number of Al atoms in the framework are balanced by Co-oxo species or not all the Co-oxo species are visible as the CT band in the region up to 50,000 cm^{-1}, the limiting frequency of the diffuse reflectance spectrometers.

The most important condition for application of the SCR–NO_x process is a high and stable activity in SCR–NO_x under the conditions in the real exhaust gases containing approx. 10% water vapour in the stream. For the analysis of the activity of Co species, it should be pointed out that the SCR–NO_x reaction is a complex process with numerous subsequent steps, each of which can affect the final conversion of NO_x to nitrogen. In the following discussion, we omitted the contribution of Al-Lewis sites (cooperating with trace concentrations of Fe) to the SCR–NO_x in dry streams and concentrated on Co-BEA* samples with high Co loadings close to $Co/Al_{FR} = 0.5$ and the SCR–NO_x process under conditions of wet NO_x streams.

From analysis of the NO_x activity of Co-BEA* zeolites exhibiting quite different distribution of framework aluminium, and thus the high population of Co_{2Al} ions (Co-BEA*-II and Co-BEA*-III) and predominant population of Co_{1Al} (Co-BEA*-IV), it follows that the bare exchanged Co(II) ions yield rather low NO_x conversion not exceeding 21% under the given conditions (see Tables 1–3, and Figs. 4 and 5) and low TOF_{total} 0.2–0.3 h^{-1}. On contrary, Co-BEA*-IV with predominant concentration of isolated Al atoms balancing the Co-oxo species provides high conversion of NO_x (90%) already at much lower Co concentration (~2 wt.%) and reaches TOF_{total} 1.9 h^{-1} and TOF_{1Al} of 3.6 h^{-1}.

The results clearly indicated dramatically higher activity of Co species in Co-BEA*-IV compared to the other Co-BEA* zeolites: (i) the most active sites for SCR–NO_x/H_2O are populated at high Co concentrations and (ii) Co-oxo species charge-balanced by isolated Al atoms in the framework are much more active compared to the low active bare Co(II) ions balanced by Al pairs.

TOF_{1Al} 2.2–2.7 h^{-1} per Co-oxo species charge-balanced by isolated Al atoms are in very good agreement with the TOF value (2.3 h^{-1}) per active Co-oxo species obtained for the series of $CoNH_4$-BEA* tested under the same conditions in [11]. The concentrations of Co-oxo active species in Ref. [11] were calculated as those not adsorbing basic acetonitrile, and presumably also water molecules. Thus different approaches, i.e. adsorption of basic molecules on Co species and analysis of Co species adjacent to isolated Al to identify the most active Co sites, provided an excellent agreement in TOF values.

In addition to the finding of the high activity of the Co-oxo species balanced by isolated framework Al atoms, a considerable transient behaviour of NO_x conversion under addition/removal of water over Co-BEA*-I and -IV zeolites, particularly at high NO_x conversions, was observed (see Figs. 6 and 7). This behaviour could be explained by water acting either in changing the structure of the Co species or by enhancement of the rate of some of the reaction step(s). Referring to the *in situ* FTIR study of Shichi et al. [60], the results on stable NO_x conversion of 90% decreasing to 40% for Co-BEA*-IV in the absence of water vapour and reversible attainment of the original conversion after water addition to the feed could be explained by their suggestion about the self-deactivation of the zeolite by CN- and CNO-intermediates and after addition of water by the increased rate of their hydrolysis to ammonia species further readily reacting with NO_x to molecular nitrogen. Nevertheless, we could not exclude the effect of reversible altering the structure of the Co species. As this behaviour was observed only for Co-BEA*-I and Co-BEA*-IV containing Co-oxo species and not for Co-zeolites containing almost exclusively bare Co(II) ions balanced by Al pairs, we can connect this behaviour with the Co-oxo species. However, analysis of this effect relative to the structure changes of the Co species requires further *in situ* spectral study.

Comparison of the concentration of Co-oxo species balanced by isolated Al atoms and the total concentration of isolated Al atoms in the parent H-BEA*-IV sample (Tables 1 and 2) indicates that only approx. 30% of the isolated Al atoms were utilized to balance the Co-oxo species. Therefore, there is still a high potential to increase the population of the active Co-oxo species in this zeolite and thus increase the SCR–NO_x activity.

Although this study did not reveal the structures of possible individual Co–O and Co–O_x Co species, the main characteristics of Co-oxo species are given. Occurrence of various structures of the counter Co-oxo species was indicated by the presence of CT Co–$O_{Ex\text{-}FR}$ transition, which, however, because of the low intensity did not correspond to the total concentration of Co-oxo species in the zeolites. As for the structure of Co-oxo species, we can only speculate that it depends on the distances of the isolated Al atoms located in two rings providing for formation of bridged Co–O_x–Co structures or stabilizing a single Co–O entity by one isolated Al atom.

Summing up, it should be stressed that the distribution of aluminium in the framework of beta zeolites dramatically changes the population of the bare Co(II) ions and Co-oxo species, balanced by Al–O–$(Si–O)_2$–Al sequences and isolated Al atoms, respectively. It has been shown that the concentration of isolated Al atoms in the framework controls the occurrence of the counter Co-oxo species, which exhibit extraordinarily high NO_x activity in real wet NO_x streams containing 10% of water vapour.

5. Conclusions

It has been shown that the distribution of aluminium in the framework dramatically affects the structure and reactivity of the counter Co ion species in beta zeolites. Al–O–$(Si–O)_2$–Al sequences in one ring and isolated Al atoms in different rings, Al–O–$(Si–O)_{n>2}$–Al sequences, occurred in the BEA* framework. While Al–O–$(Si–O)_2$–Al sequences in the framework in the cationic sites can accommodate bare Co(II) ions, the isolated Al atoms (Al–O–$(Si–O)_{n>2}$–Al sequences) located in two framework rings represent a negative charge for balancing the counter Co-oxo species.

Quantitative analysis of the concentration of bare Co(II) ions and Co-oxo species using the ^{29}Si MAS NMR and UV–Vis spectra of the Co(II) ions and estimation of the distribution of the Al atoms in the framework between the Al pairs and isolated Al atoms enabled evaluation of the concentrations and activities of the counter bare Co(II) and Co-oxo species. Compared to the bare Co(II) ions, exhibiting SCR–NO_x activity only in the absence of water vapour, the Co-oxo species exhibit high and stable activity in propane–SCR–NO_x in the presence of water (10%) in the NO_x streams. The activity likely originates from the high redox ability of the Co-oxo species due to bonding of extra-framework oxygen atom(s) and the absence of adsorption of basic molecules like water.

In addition to analysis of the structure vs. activity relationship for Co species in BEA* zeolites, the synthesis of a BEA* zeolite containing predominant concentration of isolated Al atoms in two framework rings at relatively high concentration of framework aluminium (Si/Al 15) is reported. This zeolite with a high concentration of isolated Al atoms (~60% of framework Al) is able to stabilize a high concentration of highly active Co-oxo species. As these species do not adsorb basic molecules and accordingly also water molecules, they yield high NO_x conversions in real NO_x streams containing 10% of water vapour. While the bare exchanged Co(II) ions exhibit very low activity under these conditions, the Co-oxo species attain TOF_{1Al} per Co-oxo species of around 3–4 h^{-1}.

Summing up, we can state that the controlled distribution of aluminium in the beta framework by the procedure of zeolite synthesis or post-synthesis treatment can govern the concentration of bare Co(II) cations accommodated by the Al–O–$(Si–O)_2$–Al sequences in the cationic sites or Co-oxo species in the vicinity of isolated Al atoms. This study provided evidence for the superior activity of the counter Co-oxo species in beta zeolites adjacent to isolated Al atoms in SCR–NO_x streams containing high concentrations of water vapour. Analogous behaviour can be expected for the other multivalent cations with respect to the distribution of framework aluminium. This finding might provide for tailoring of the redox activity of metal-zeolite catalysts in various redox reactions.

Acknowledgments

The authors thank for the financial support to Academy of Sciences under the Project # KAN100400702 and # IAA400400904, and to the EU Network of Excellence IDECAT # NMP 3-CT-2005-011730.

Appendix A. Supplementary material

Supplementary data associated with this article can be found, in the online version, at doi:10.1016/j.jcat.2010.03.013.

References

[1] B. Wichterlova, J. Dedecek, Z. Sobalik, Catalysis by Unique Metal Ion Structures in Solid Matrices: From Science to Application 13 (2001) 31.
[2] B. Wichterlova, Top. Catal. 28 (2004) 131.
[3] Z. Sobalik, J. Dedecek, I. Ikonnikov, B. Wichterlova, Micropor. Mesopor. Mater. 21 (1998) 525.
[4] M. Iwamoto, S. Yokoo, K. Sakai, S. Kagawa, J. Chem. Soc. Faraday Trans. I 77 (1981) 1629.
[5] Y. Kuroda, T. Mori, Y. Yoshikawa, S. Kittaka, R. Kumashiro, M. Nagao, Phys. Chem. Chem. Phys. 1 (1999) 3807.
[6] M. Iwamoto, H. Hamada, Catal. Today 10 (1991) 57.
[7] M. Iwamoto, H. Yahiro, Catal. Today 22 (1994) 5.
[8] Y.J. Li, P.J. Battavio, J.N. Armor, J. Catal. 142 (1993) 561.
[9] B. Wichterlová, J. Dedecek, Z. Sobalík, A. Vondrová, K. Klier, J. Catal. 169 (1997) 194.
[10] T.V. Voskoboinikov, H.Y. Chen, W.M.H. Sachtler, Appl. Catal. B 19 (1998) 279.
[11] L. Capek, J. Dedecek, B. Wichterlova, J. Catal. 227 (2004) 352.
[12] A. Itadani, Y. Kuroda, M. Tanaka, M. Nagao, Micropor. Mesopor. Mater. 86 (2005) 159.
[13] W.J. Mortier, J. Phys. Chem. 81 (1977) 1334.
[14] J. Elsen, G.S.D. King, W.J. Mortier, J. Phys. Chem. 91 (1987) 5800.
[15] D. Kaucky, J. Dedecek, B. Wichterlova, Micropor. Mesopor. Mater. 31 (1999) 75.
[16] J. Dedecek, B. Wichterlova, J. Phys. Chem. B 103 (1999) 1462.
[17] J. Dedecek, D. Kaucky, B. Wichterlova, Micropor. Mesopor. Mater. 35 (6) (2000) 483.
[18] J. Dedecek, L. Capek, D. Kaucky, Z. Sobalik, B. Wichterlova, J. Catal. 211 (2002) 198.
[19] L. Drozdova, R. Prins, J. Dedecek, Z. Sobalik, B. Wichterlova, J. Phys. Chem. B 106 (2002) 2240.
[20] M.C. Dalconi, G. Cruciani, A. Alberti, P. Ciambelli, M.T. Rapacciuolo, Micropor. Mesopor. Mater. 39 (2000) 423.
[21] M.C. Dalconi, A. Alberti, G. Cruciani, J. Phys. Chem. B 107 (2003) 12973.
[22] M.C. Dalconi, A. Alberti, G. Cruciani, P. Ciambelli, E. Fonda, Micropor. Mesopor. Mater. 62 (2003) 191.
[23] H. Ohtsuka, T. Tabata, O. Okada, L.M.F. Sabatino, G. Bellussi, Catal. Today 42 (1998) 45.
[24] K. Gora-Marek, B. Gil, J. Datka, Appl. Catal. A 353 (2009) 117.
[25] H.Y. Chen, W.M.H. Sachtler, Catal. Today 42 (1998) 73.
[26] M. Iwamoto, H. Yahiro, H.K. Shin, M. Watanabe, J.W. Guo, M. Konno, T. Chikahisa, T. Murayama, Appl. Catal. B 5 (1994) L1.
[27] T. Tabata, H. Ohtsuka, L.M.F. Sabatino, G. Bellussi, Micropor. Mesopor. Mater. 21 (1998) 517.
[28] D. Kaucky, A. Vondrova, J. Dedecek, B. Wichterlova, J. Catal. 194 (2000) 318.
[29] Y. Li, J.N. Armor, Appl. Catal. B 3 (1993) L1.
[30] T. Tabata, M. Kokitsu, H. Ohtsuka, O. Okada, L.M.F. Sabatino, G. Bellussi, Catal. Today 27 (1996) 91.
[31] O. Okada, T. Tabata, M. Kokitsu, H. Ohtsuka, L.M.F. Sabatino, G. Bellussi, Appl. Surf. Sci. 121 (1997) 267.
[32] H. Ohtsuka, T. Tabata, O. Okada, L.M.F. Sabatino, G. Bellussi, Catal. Lett. 44 (1997) 265.
[33] P. Sarv, C. Fernandez, J.P. Amoureux, K. Keskinen, J. Phys. Chem. 100 (1996) 19223.
[34] J. Dedecek, D. Kaucky, B. Wichterlova, Chem. Commun. (2001) 970.
[35] J. Dedecek, D. Kaucky, B. Wichterlova, O. Gonsiorova, Phys. Chem. Chem. Phys. 4 (2002) 5406.
[36] O.H. Han, C.S. Kim, S.B. Hong, Angew. Chem. Int. Ed. 41 (2002) 469.
[37] V. Gabova, J. Dedecek, J. Cejka, Chem. Commun. (2003) 1196.
[38] L. Capek, J. Dedecek, B. Wichterlova, L. Cider, E. Jobson, V. Tokarova, Appl. Catal. B 60 (2005) 147.
[39] M. Derewinski, P. Sarv, A. Mifsud, Catal. Today 114 (2006) 197.
[40] J. Dedecek, L. Capek, B. Wichterlova, Appl. Catal. A 307 (2006) 156.
[41] S. Sklenak, J. Dedecek, C.B. Li, B. Wichterlova, V. Gabova, M. Sierka, J. Sauer, Angew. Chem. Int. Ed. 46 (2007) 7286.
[42] S. Sklenak, J. Dedecek, C. Li, B. Wichterlova, V. Gabova, M. Sierka, J. Sauer, Phys. Chem. Chem. Phys. 11 (2009) 1237–1247.
[43] J.A. Van Bokhoven, T.L. Lee, M. Drakopoulos, C. Lamberti, S. Thiss, J. Zegenhagen, Nat. Mater. 7 (2008) 551.
[44] J. Dedecek, S. Sklenak, C. Li, B. Wichterlova, V. Gabova, J. Brus, M. Sierka, J. Sauer, J. Phys. Chem. C 113 (2009) 1447.
[45] P. Sazama, J. Dedecek, V. Gabova, B. Wichterlova, G. Spoto, S. Bordiga, J. Catal. 254 (2008) 180.
[46] E.J. Creyghton, S.D. Ganeshie, R.S. Downing, H. van Bekkum, J. Mol. Catal. A 115 (1997) 457.
[47] Patent pending CZ 2010-91.
[48] C.A. Fyfe, Y. Feng, H. Grondey, G.T. Kokotailo, H. Gies, Chem. Rev. 91 (1991) 1525.
[49] B. Wichterlova, Z. Tvaruzkova, Z. Sobalik, P. Sarv, Micropor. Mesopor. Mater. 24 (1998) 223.
[50] P. Sazama, L. Capek, H. Drobna, Z. Sobalik, J. Dedecek, K. Arve, B. Wichterlova, J. Catal. 232 (2005) 302.
[51] I. Kiricsi, C. Flego, G. Pazzuconi, W.O. Parker, R. Millini, C. Perego, G. Bellussi, J. Phys. Chem. 98 (1994) 4627.
[52] O. Bortnovsky, Z. Sobalik, B. Wichterlova, Micropor. Mesopor. Mater. 46 (2001) 265.
[53] Z. Sobalïk, A. Vondrova, Z. Tvaruzkova, B. Wichterlova, Catal. Today 75 (2002) 347.
[54] G.I. Pannov, V.I. Sobolev, A.S. Kharitonov, J. Mol. Catal. 61 (1990) 85.
[55] G.I. Panov, G.A. Sheveleva, A.S. Kharitonov, V.N. Romannikov, L.A. Vostrikova, Appl. Catal. A 82 (1992) 31.
[56] H.Y. Chen, E.M. El-Malki, X. Wang, R.A. van Santen, W.M.H. Sachtler, J. Mol. Catal. A 162 (2000) 159.
[57] V.M. Miskowski, J.L. Robbins, I.M. Treitel, H.B. Gray, Inorg. Chem. 14 (1975) 2318.
[58] A.B.P. Lever, H.B. Gray, Acc. Chem. Res. 11 (1978) 348.
[59] V.M. Miskowski, B.D. Santarsiero, W.P. Schaefer, G.E. Ansok, H.B. Gray, Inorg. Chem. 23 (1984) 172.
[60] A. Shichi, T. Hattori, A. Satsuma, Appl. Catal. B 77 (2007) 92.